

Supporting Information

Multi-Responsive Nanogels with Tunable Orthogonal Reversible Covalent (TORC) Core-Crosslinks for AND-Gate Controlled Release

Shayesteh Tafazoli,^a Ali Shahrokhinia,^a Sahaj Rijal,^a Jaelese Garay,^a Randall A. Scanga,^a James F. Reuther^a*

^a Department of Chemistry, University of Massachusetts Lowell, Lowell, MA 01854

Table of Content

1. Equipment
2. Small Molecule/Crosslinker Synthesis and Characterization
3. Synthesis and Characterization of PGMA-based TORC-NGs
4. Multi-Stimuli Responsiveness of TORC-NGs
5. Sequential Application of Stimuli for AND-Gate release
6. Characterization and Nile Red Release for Tubesome TORC-NGs
7. References

1. Equipment

1.1. NMR spectroscopy

The ^1H and ^{13}C nuclear magnetic resonance (NMR) spectra were obtained on a JEOL ECZ 400 MHz spectrometer, employing CDCl_3 and DMSO-d_6 (Sigma-Aldrich) as solvents and referencing them to residual solvent signals. The ^1H NMR spectra were acquired with an average of 16 scans. To investigate the kinetics of the reaction, 10 mol% of DMF was included in the reaction mixture as an internal standard enabling the monitoring of monomer consumption throughout the reaction duration.

1.2. Gel permeation chromatography (GPC)

The molecular weight (M_n) and molecular weight distribution (M_w/M_n) were determined by employing an Tosoh HLC8320 EcoSEC GPC system. This system was equipped with a refractive index (RI) detector, operating at a temperature of 40 °C. The styragel column were calibrated using monodispersed polystyrene standards and HPLC-grade tetrahydrofuran (THF) was used as the eluent at a rate of 0.5 mL/min. All chromatographic runs had a duration of 10 minutes.

1.3. Transmission Electron Microscopy (TEM)

Transmission electron microscopy (TEM) was conducted using a Philips CM12 electron microscope operating at 120 kV. The polymerization dispersions were diluted with methanol to concentration = 1.0 mg/mL, and the resulting dispersions were drop-casted onto carbon-coated copper grids (Ted Pella). Subsequently, the grids were dried in a vacuum oven. The TEM imaging of all samples was performed without the use of any external staining agents.

1.4. Dynamic light scattering (DLS)

To determine the average hydrodynamic diameters and size distribution of nanoparticles, dynamic light scattering (DLS) was performed using a Horiba SZ-100 Particle Analyzer. The scattered light was detected at an angle of 90°. The samples were prepared by dissolving copolymers in desired solvents, which were filtered and adjusted to a concentration of 5.0 mg/mL at a temperature of 25 °C. Data processing was carried out utilizing the general-purpose algorithms available in the SZ-100 Software. To ensure accuracy, triple runs were conducted for each sample, and the results were reported as an average.

1.5. Fluorescence spectroscopy

Fluorescence spectra of TORC-NG samples encapsulated with Nile Red were acquired using a JASCO FP-8500 fluorescence spectrophotometer. The excitation and emission wavelengths were set at 540 nm and 630 nm, respectively. The measurements were conducted at ambient temperature with a sample concentration of 5.0 mg/ml.

1.6. UV-Vis Spectroscopy

UV-Vis spectra were obtained using a Hach DR 6000EDU UV-Vis spectrophotometer utilizing quartz cuvettes with a path length of 10 mm. The spectra were scanned in the range of $\lambda = 200$ to 500 nm.

2. Small Molecule/Crosslinker Synthesis and Characterization

Synthesis of 7-(2-hydroxyethoxy)-4-methylcoumarin

The synthesis procedure was adapted from previously reported literature,¹ except the product was obtained after three recrystallization cycles from ethyl acetate/methanol (8:2, v:v).

¹H NMR (400 MHz, DMSO-d₆) δ = 7.63 (d, J = 9.4 Hz, 1H), 6.91-6.94 (m, 2H), 6.17 (s, 1H), 4.95 (broad), 4.05 (t, J = 4.8 Hz, 2H), 3.70 (t, J = 4.7 Hz, 2H), 2.35 (s, 3H).

Synthesis of 7-(2-methacryloyloxyethoxy)-4-methylcoumarin

The procedure was adapted from previously published literature.¹

¹H NMR (400 MHz, CDCl₃) δ = 7.51 (d, J = 8.9 Hz, 1H), 6.84-6.95 (m, 2H), 6.16 (s, 2H), 5.61 (t, J = 1.3 Hz, 1H), 4.48-4.59 (m, 2H), 4.28-4.34 (m, 2H), 2.35-2.47 (m, 3H), 1.96 (s, 3H).

Synthesis of N,N-Cystaminebismethacrylamide (CBMA) crosslinker

The synthesis of CBMA was adapted from previously reported literature protocols.²

Synthesis of alkyne-ATRP initiator

The synthesis of CBMA was adapted from previously reported literature protocols.³

3. Synthesis and Characterization of PGMA-based TORC-NGs

3.1. Synthesis and Characterization of POEGMA-grad-PGMA gradient copolymer

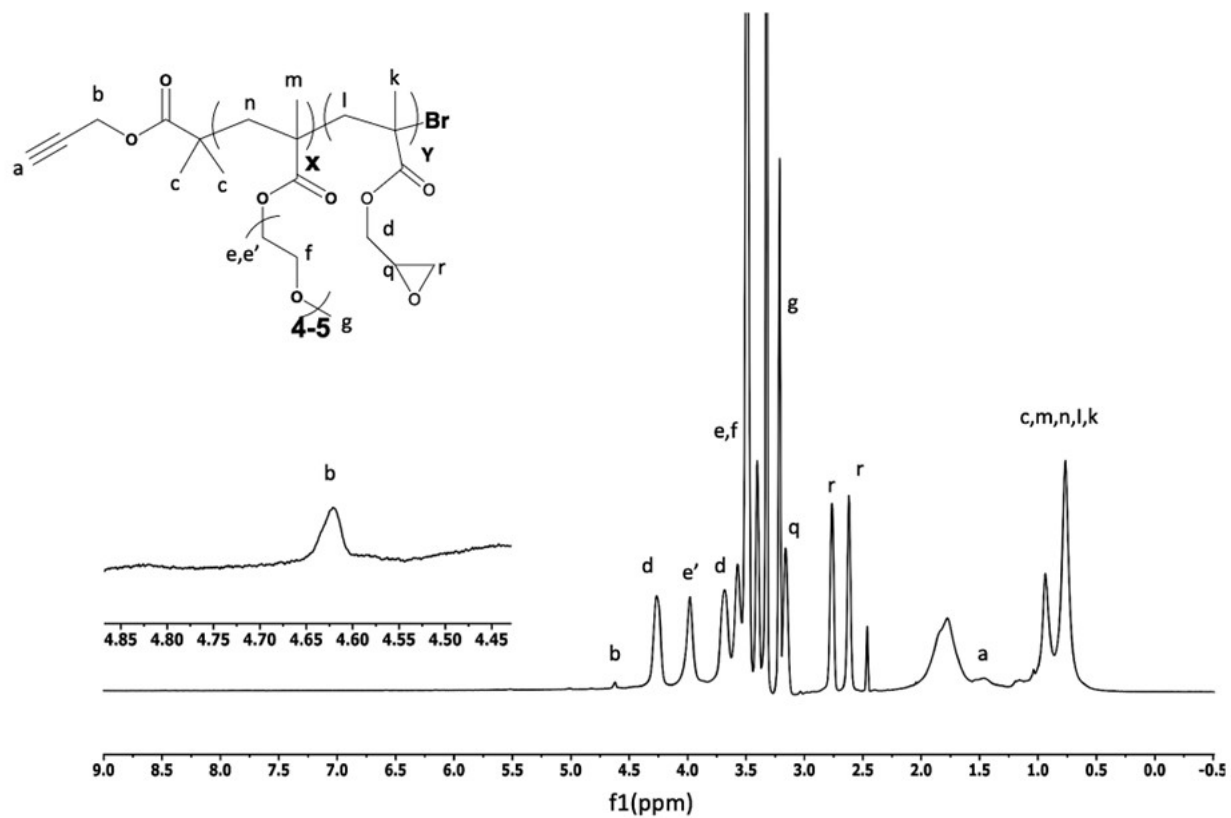


Figure S1. ¹H NMR spectrum of the POEGMA-grad-PGMA gradient copolymer formed via PhotoATR-PISA for control non-CCL nanospheres (target DP(PGMA) = 86; SC% = 25%).

3.2. Synthesis and Characterization of Spherical TORC-NG

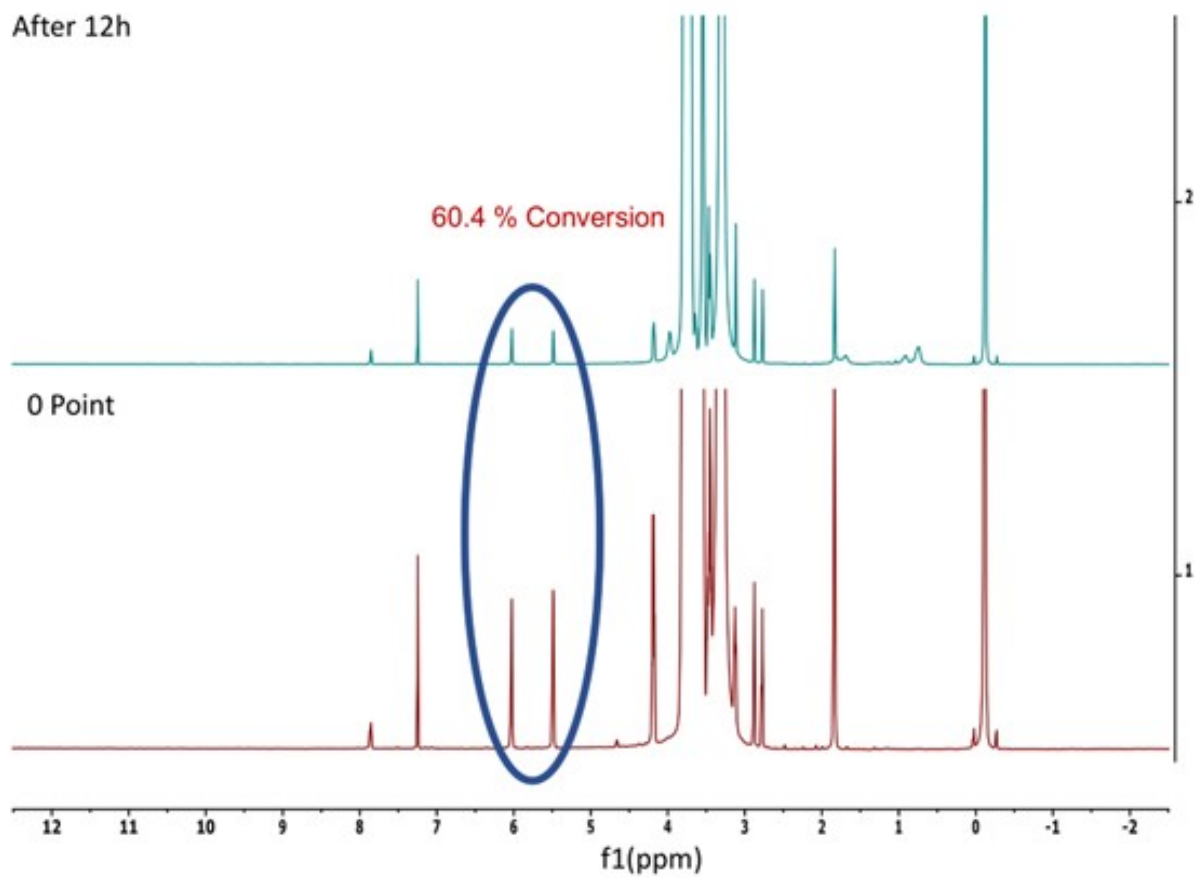


Figure S2. ¹H NMR spectra for POEGMA macroinitiator in the synthesis of spherical TORC-NG at t_0 and after 12 h reaction showing ~60% OEGMA conversion.

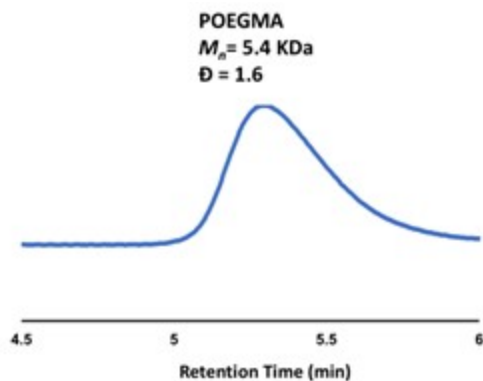


Figure S3. GPC chromatogram of POEGMA macroinitiator used in the synthesis of spherical TORC-NG after 12 h reaction and 60% conversion

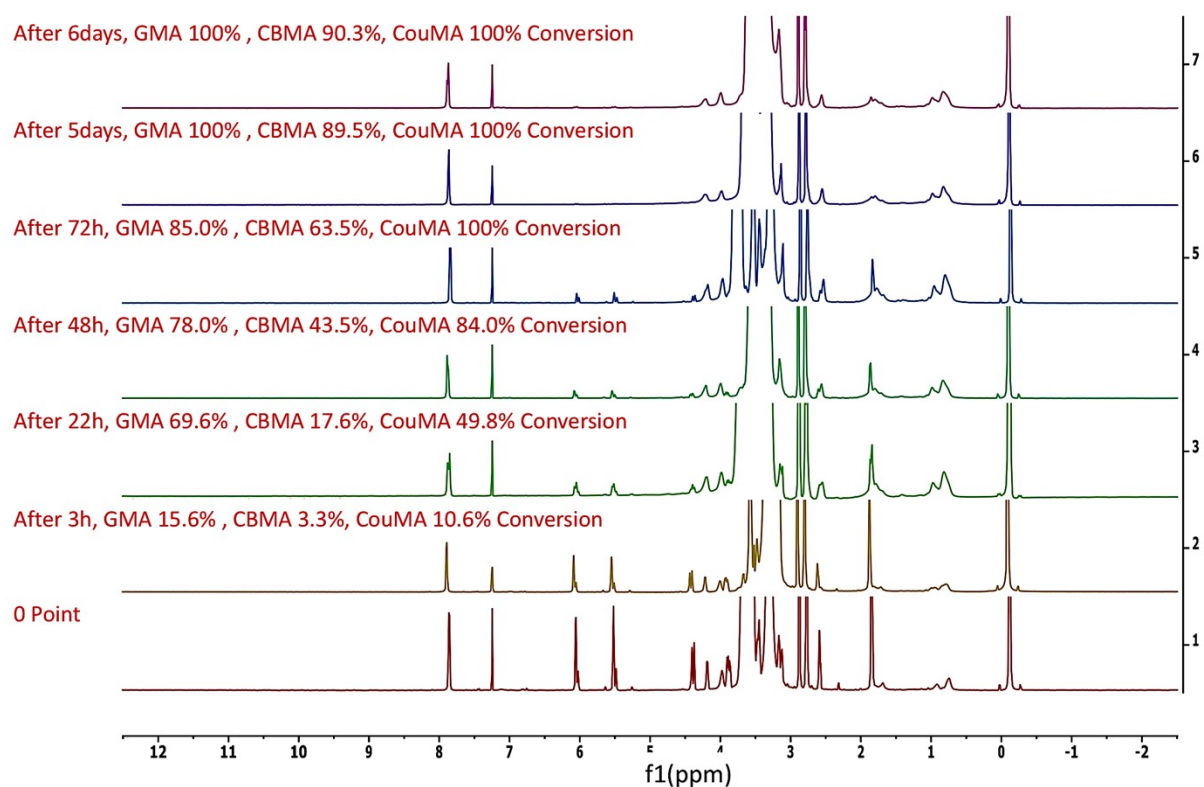


Figure S4. Kinetics of GMA, CBMA and CouMA polymerizations for spherical TORC-NGs as a function of time analyzed using ^1H NMR spectroscopy using integrations of monomer peaks with respect to DMF internal standard.

3.3. Synthesis and Characterization of Worm-like TORC-NG

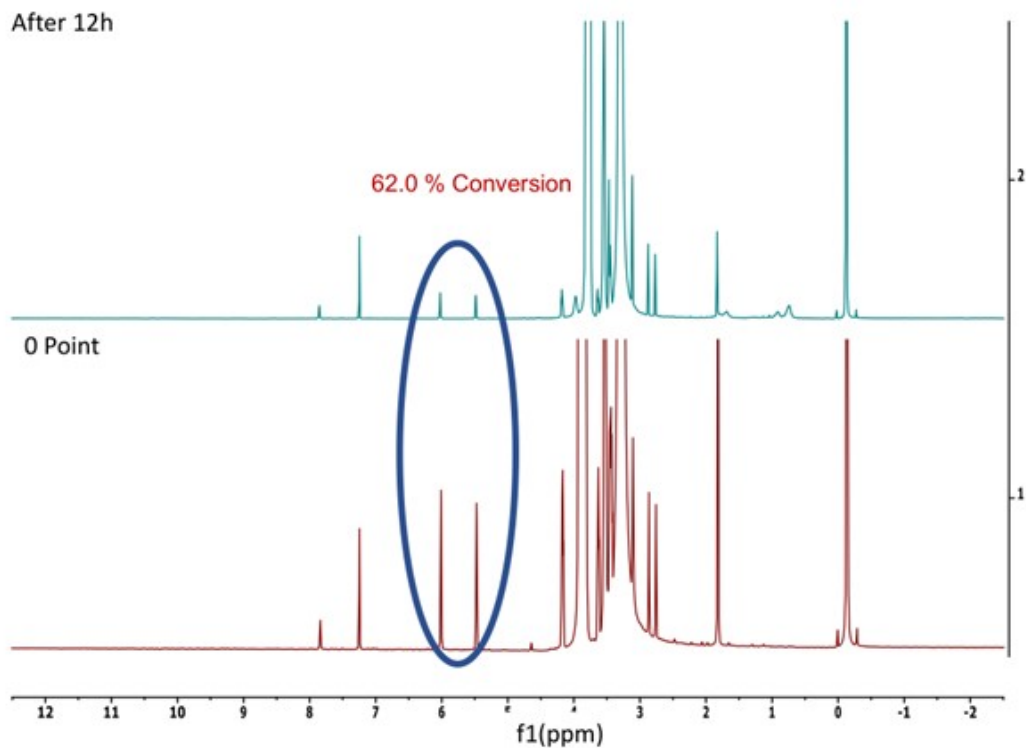


Figure S5. ¹H NMR spectra for POEGMA macroinitiator in the synthesis of worm-like TORC-NG at t_0 and after 12 h reaction showing 62% OEGMA conversion.

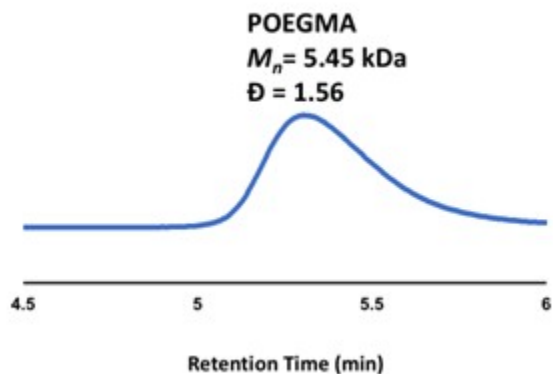


Figure S6. GPC chromatogram of POEGMA macroinitiator used in the synthesis of worm-like TORC-NG after 12 h reaction and 62% conversion.

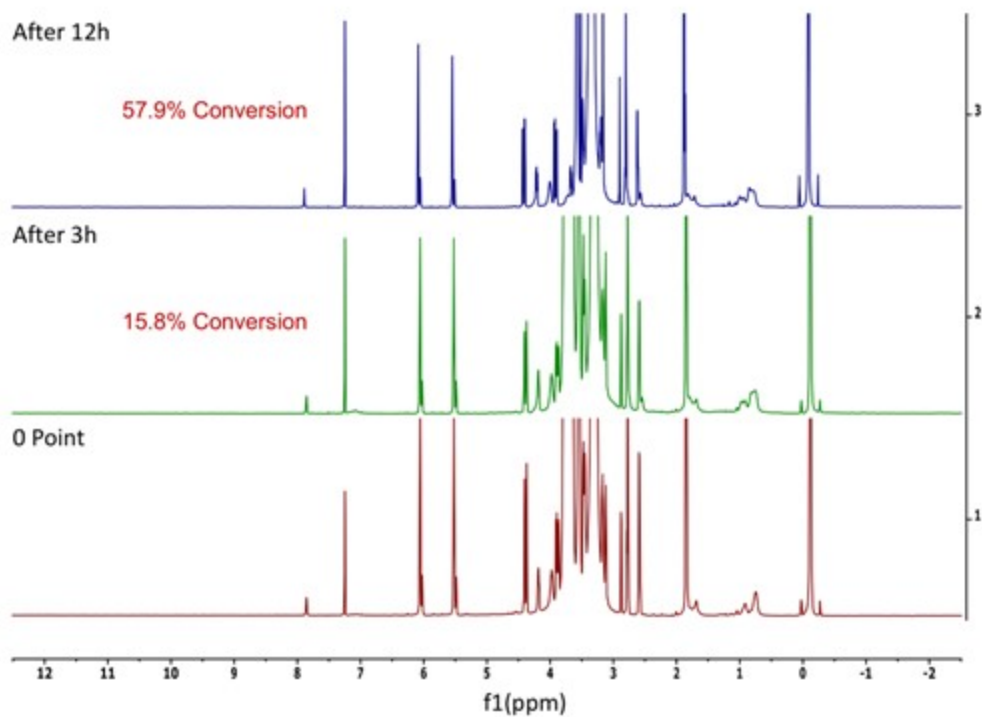


Figure S7. ^1H NMR spectra for PGMA in the synthesis of worm-like TORC-NG at t_0 and after 3, and 12 h reaction conducted to monitor conversion of first addition of GMA.

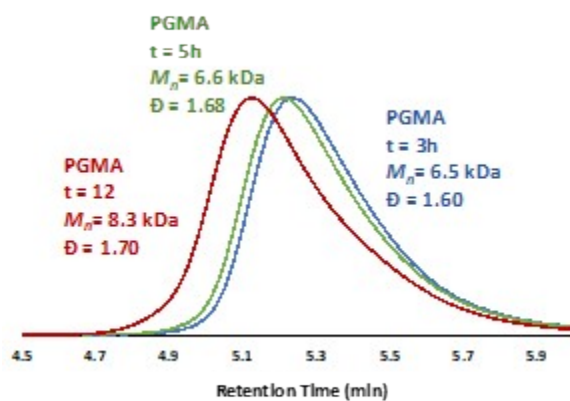


Figure S8. GPC chromatogram of PGMA (prior to TORC-CCL) used in the synthesis of worm-like TORC-NG monitored over time during 12 h reaction.

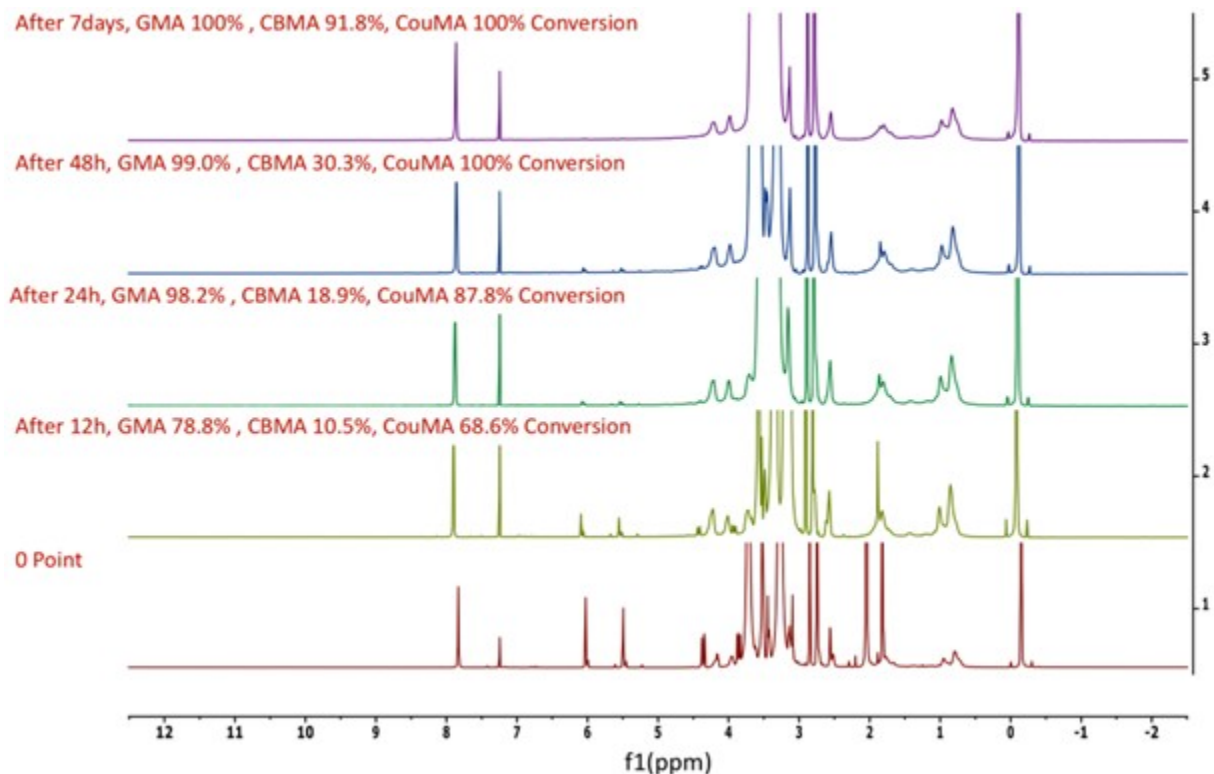


Figure S9. The progress of GMA and crosslinker conversion for worm-like TORC-NG was monitored using ^1H NMR spectroscopy over a period of 7 days. The obtained results indicated complete conversion for GMA, while CouMA and CBMA exhibited conversions of 100% and 91.8% respectively.

3.4. Polymer and Nile Red Stability under UV-C Irradiation

To induce decrosslinking of the CouMA moiety, all TORC-NG particles were subjected to 254 nm UV light irradiation for 1 h. A series of experiments was designed to explore the impact of UV-C radiation on the polymeric and Nile Red stability to ensure no photodegradation. Initially, homopolymers of each block, namely POEGMA (hydrophilic stabilizer) and PGMA (hydrophobic core), were synthesized. Subsequently, block copolymers of the same without the inclusion of

Nile Red were also prepared. These samples were then exposed to UV-C irradiation and samples were analyzed via ^1H NMR and GPC over the course of 1 h.

As illustrated in **Figure S10-15**, the integrity of the polymeric backbone (as determined by ^1H NMR) and the molecular weight (as assessed by GPC) remained consistent throughout the experimental duration. This observation demonstrates that all homopolymers and copolymers exhibited complete stability in the presence of 254 nm UV-C radiation over the course of irradiation (1 h). Furthermore, the photostability of Nile Red was assessed while dissolved in DMF and irradiated for 1 h showing minimal reduction in fluorescence intensity demonstrating limited amounts of photo-bleaching occurring during this process. Importantly, this data indicates that the reduction in fluorescence intensity observed experimentally is primarily attributed to the decrosslinking of the CouMA and release of Nile Red cargo rather than degradation of the polymeric backbone.

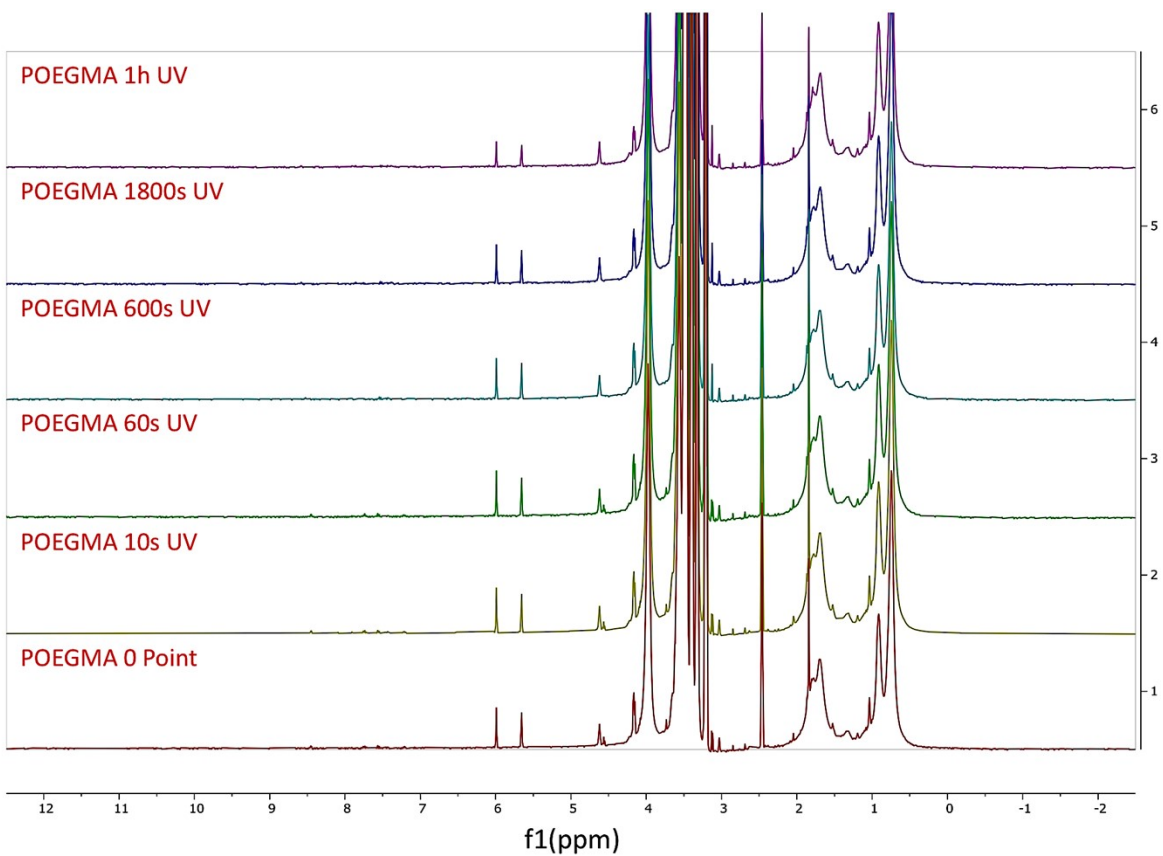


Figure S10. ^1H NMR spectra for POEGMA homopolymer control showing no changes upon UV-C irradiation over the course of 1 h.

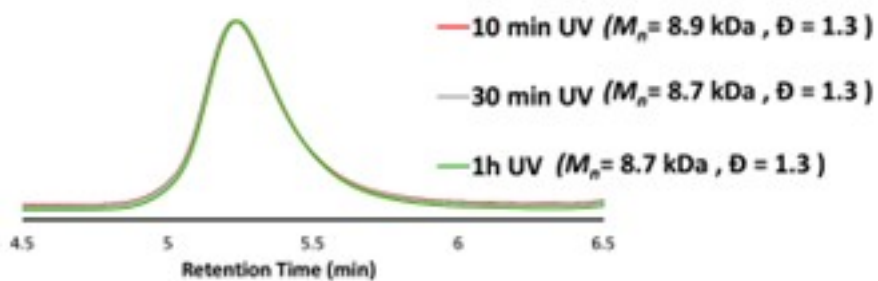


Figure S11. GPC for POEGMA homopolymer control showing no changes upon UV-C irradiation over the course of 1 h.

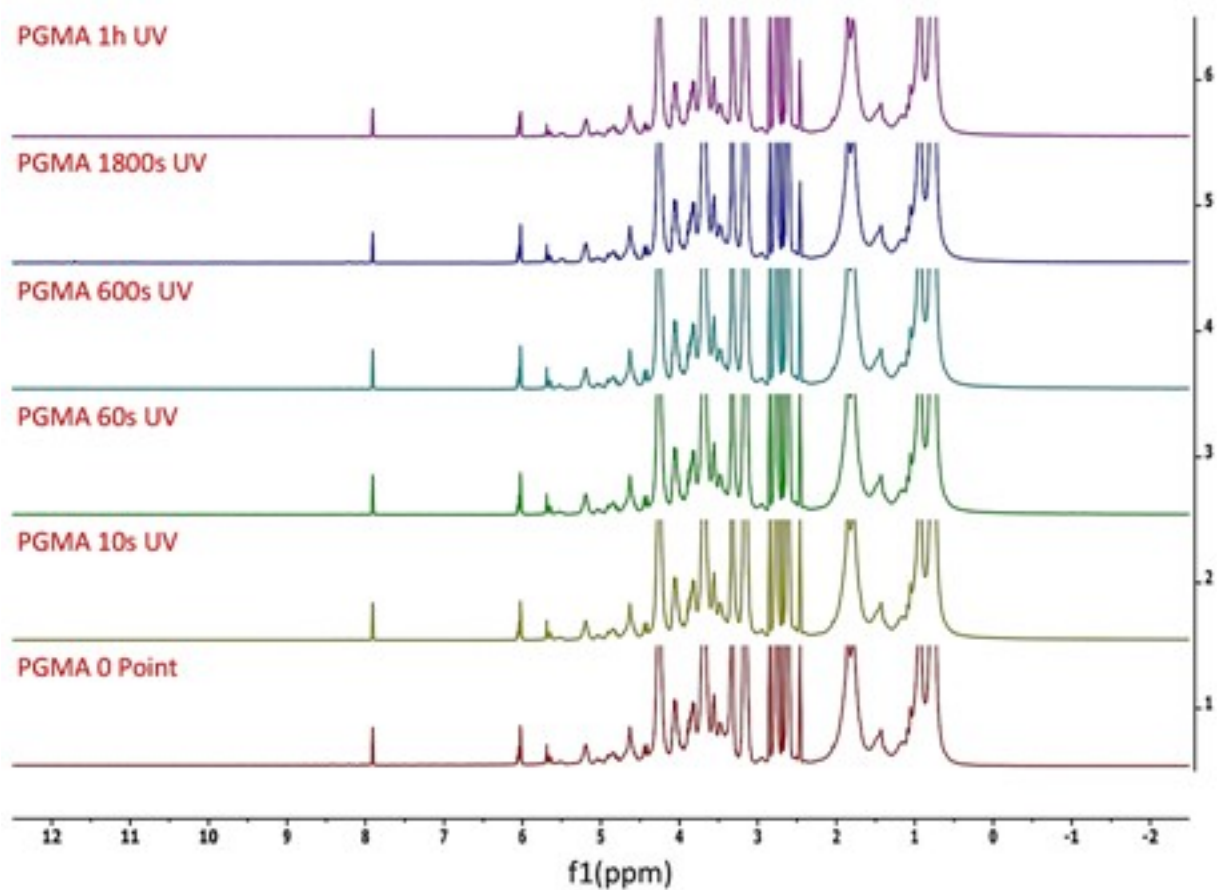


Figure S12. ^1H NMR spectra for PGMA homopolymer control showing no changes upon UV-C irradiation over the course of 1 h.

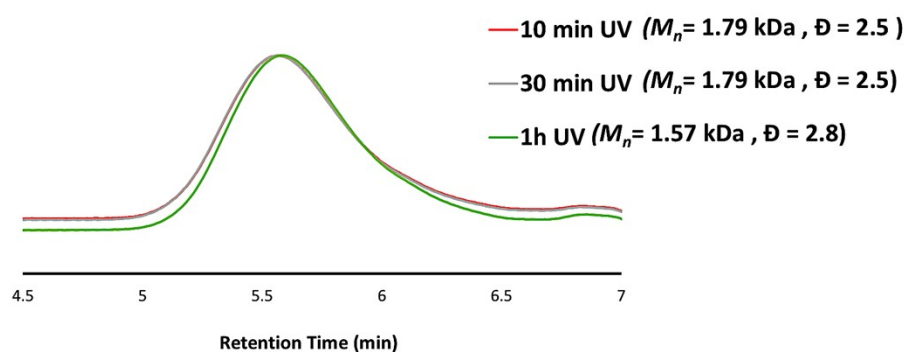


Figure S13. GPC for PGMA homopolymer control showing no changes upon UV-C irradiation over the course of 1 h.

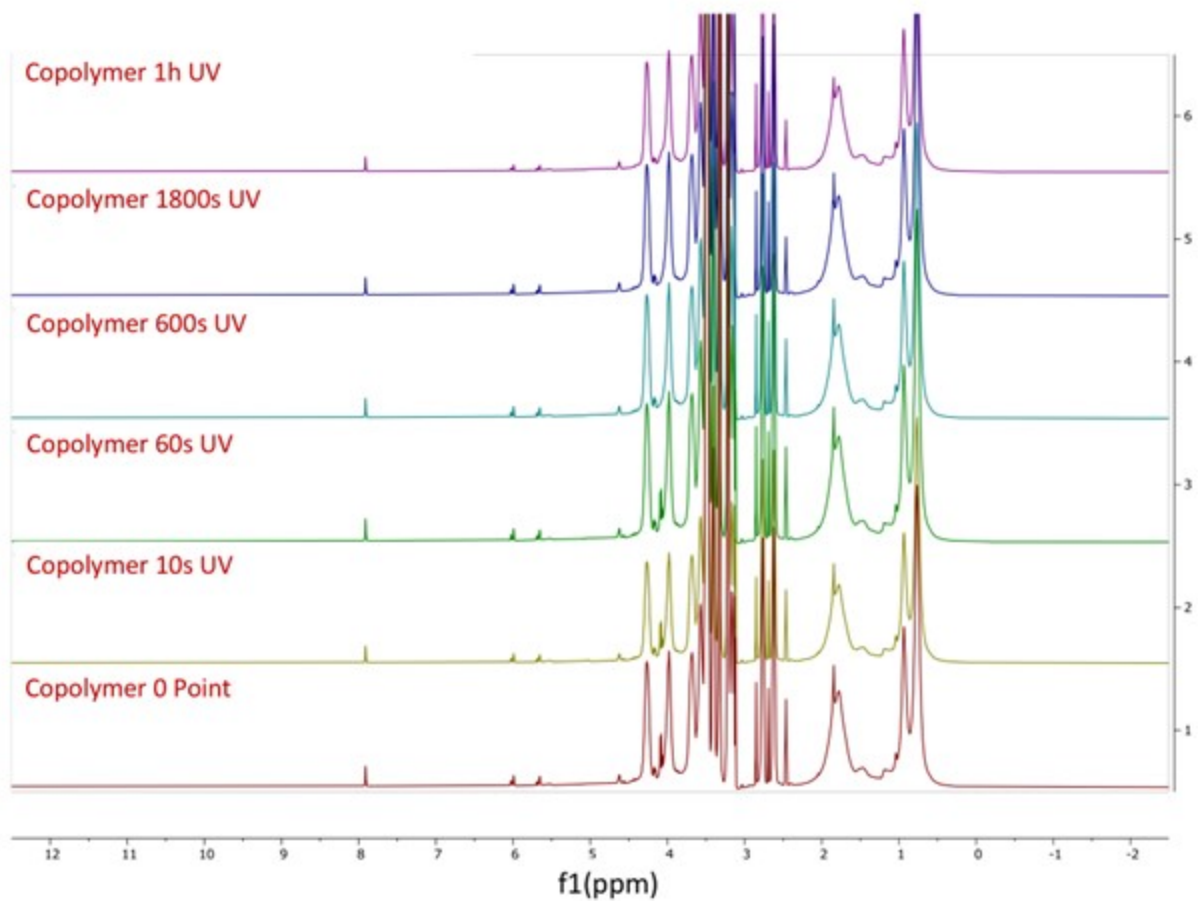


Figure S14. ^1H NMR spectra for POEGMA-b-PGMA block copolymer control showing no changes upon UV-C irradiation over the course of 1 h.

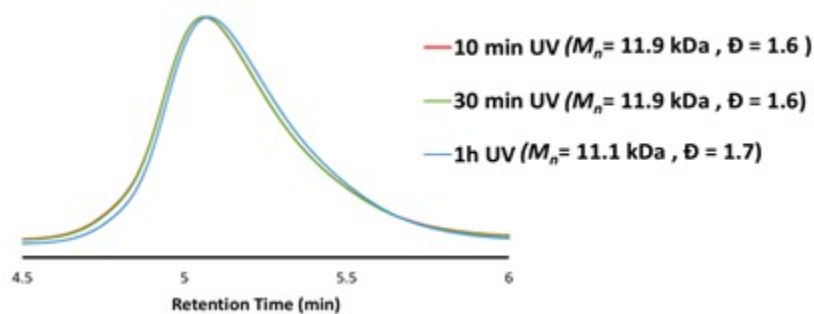


Figure S15. GPC for POEGMA-b-PGMA block copolymer control showing no changes upon UV-C irradiation over the course of 1 h.

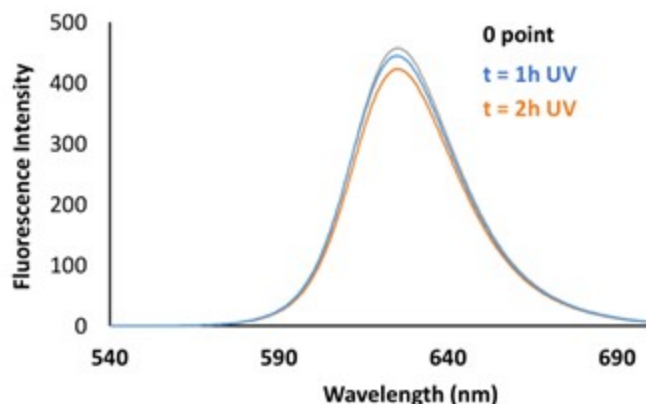


Figure S16. Fluorescence spectra of Nile Red dissolved in DMF after 1 and 2 h UV-C irradiation showing minimal photo-bleaching under the operational window of irradiation (1 h).

4. Multi-Stimuli Responsiveness of TORC-NGs

4.1. Acid-induced Solubility Switching of PGMA Cores

The present study investigates ring-opening hydrolysis reactions in the poly(glycidyl methacrylate) (PGMA) cores induced by acid incubation (pH = 4). To confirm the hypothesized reaction pathway, ^1H NMR analysis was implemented for non-CCL nanosphere materials revealing significant alterations in the epoxide chemical shifts and appearance of new peaks associated specifically for protons adjacent to the ester group (d, Figure S1) and epoxide protons (r, Figure S1). For this, peaks at 3.75 ppm (d) diminish in intensity while new peaks at 3.9 ppm (h), 4.9 and 5 ppm (f) increase intensity.

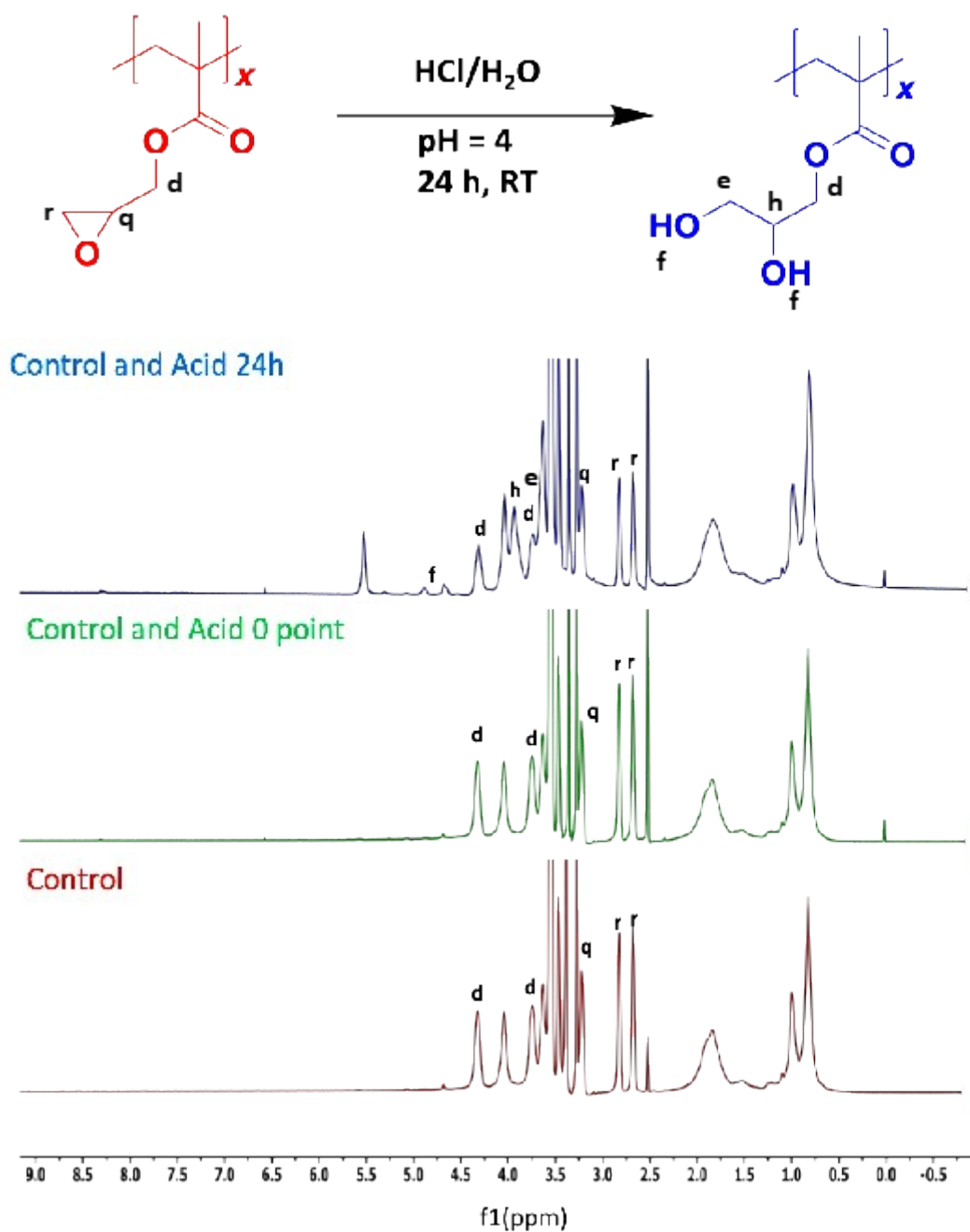


Figure S17. ^1H NMR spectra for non-CCL nanosphere control sample of POEGMA-grad-PGMA demonstrating ring-opening hydrolysis of epoxide pendants in HCl/H₂O (pH = 4) for 24 h.

4.2. De-crosslinking of CouMA under UV-C irradiation monitored via UV-Vis Spectroscopy:

The kinetics of CouMA decrosslinking via photocission was monitored using UV-Vis spectroscopy after exposure to 254 nm UV light. Free CouMA pendants (non-crosslinked) display clear absorption peaks at $\lambda_{\text{max}} = 320$ nm which disappears upon irradiation with 365 nm UV-A light during PhotoATR-PISA. The intensity of this peaked is subsequently restored upon irradiation with 254 nm UV-C light providing facile monitoring of the de-crosslinking process (Figure S18). This de-crosslinking process was confirmed upon UV-Vis analysis of spherical TORC-NG samples over the course of 1 h irradiation with 254 nm UV-C light.

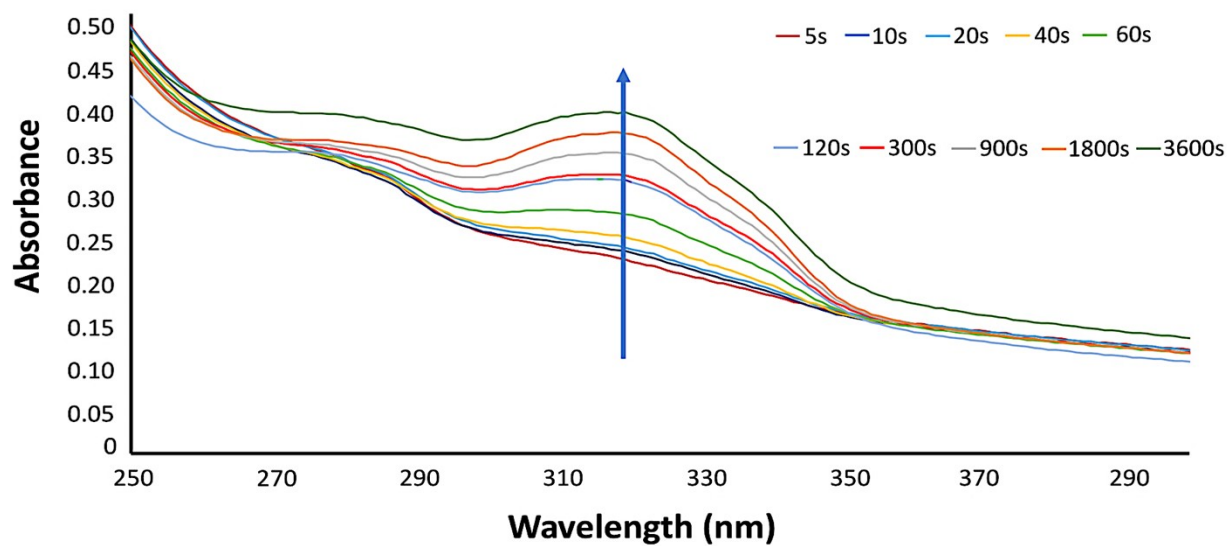


Figure S18. De-crosslinking of CouMA under UV-C irradiation for spherical TORC-NG, monitored via UV-Vis spectroscopy.

4.3. Stimuli-Induced Nile-Red Release

In the section “Multi-stimuli responsive cargo release from Nile Red-loaded TORC-NGs” of the main text, we have discussed the release of Nile red from both TORC-NG morphologies. Here the fluorescence intensity plots are used to calculate the release profile in diverse environmental conditions, each characterized by distinct stimuli responses. All fluorescence spectra were normalized in intensity to the $t = 0$ point prior to any application of stimuli to provide a necessary baseline for release. All release experiments were analyzed with (dotted lines) and without (solid lines) UV-irradiation to observe the effects of UV-induced de-crosslinking with other triggers (acidic, DTT, GSH) present simultaneously.

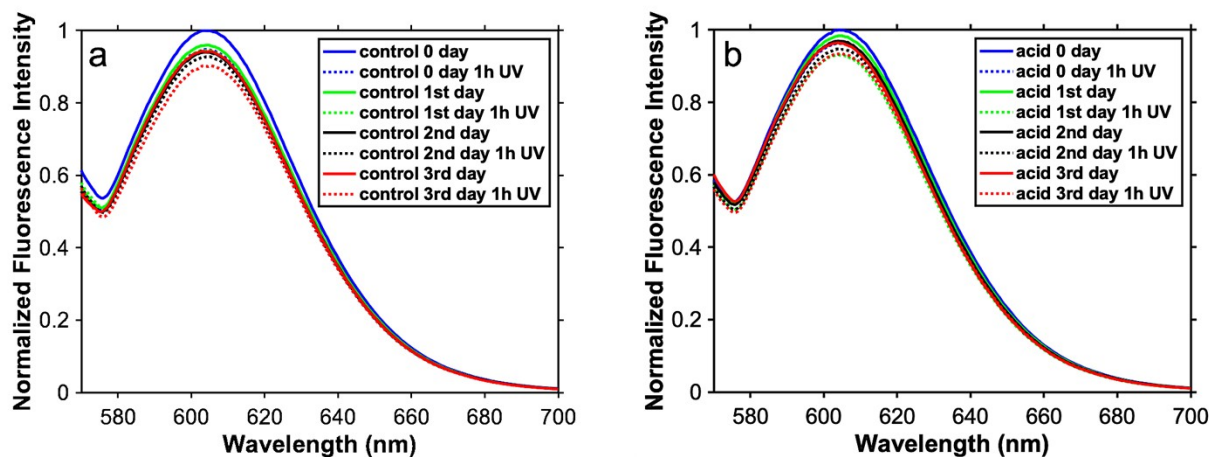


Figure S19. Fluorescence spectra of Nile Red loaded spherical TORC-NG over the course of 3 days monitoring with (dotted lines) and without (solid lines) 254 nm UV irradiation at pH = 7 (a) and acidified to pH = 4 with HCl/H₂O (b).

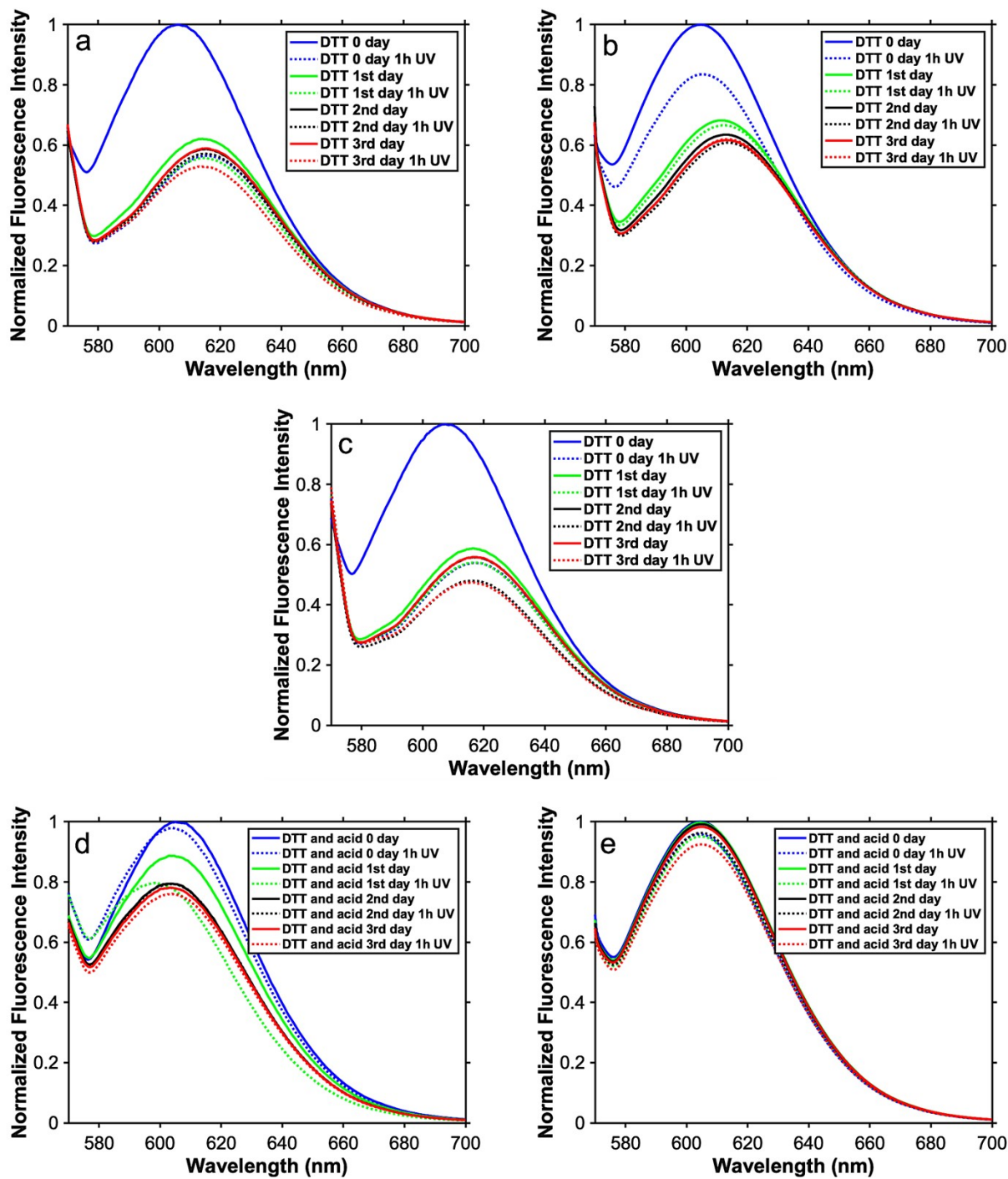


Figure S20. The fluorescence spectra of Nile Red loaded spherical TORC-NGs upon exposure to dithiothreitol (DTT) at various concentrations. The molar ratios of DTT to CBMA are as follows: (a) DTT:CBMA = 64:1, (b) DTT:CBMA = 16:1, and (c) DTT:CBMA = 128:1. Additionally, the redox

responsiveness was evaluated upon acidification to pH = 4 with HCl/H₂O at two different DTT concentrations: (d) DTT:CBMA = 64:1 and (e) DTT:CBMA = 16:1.

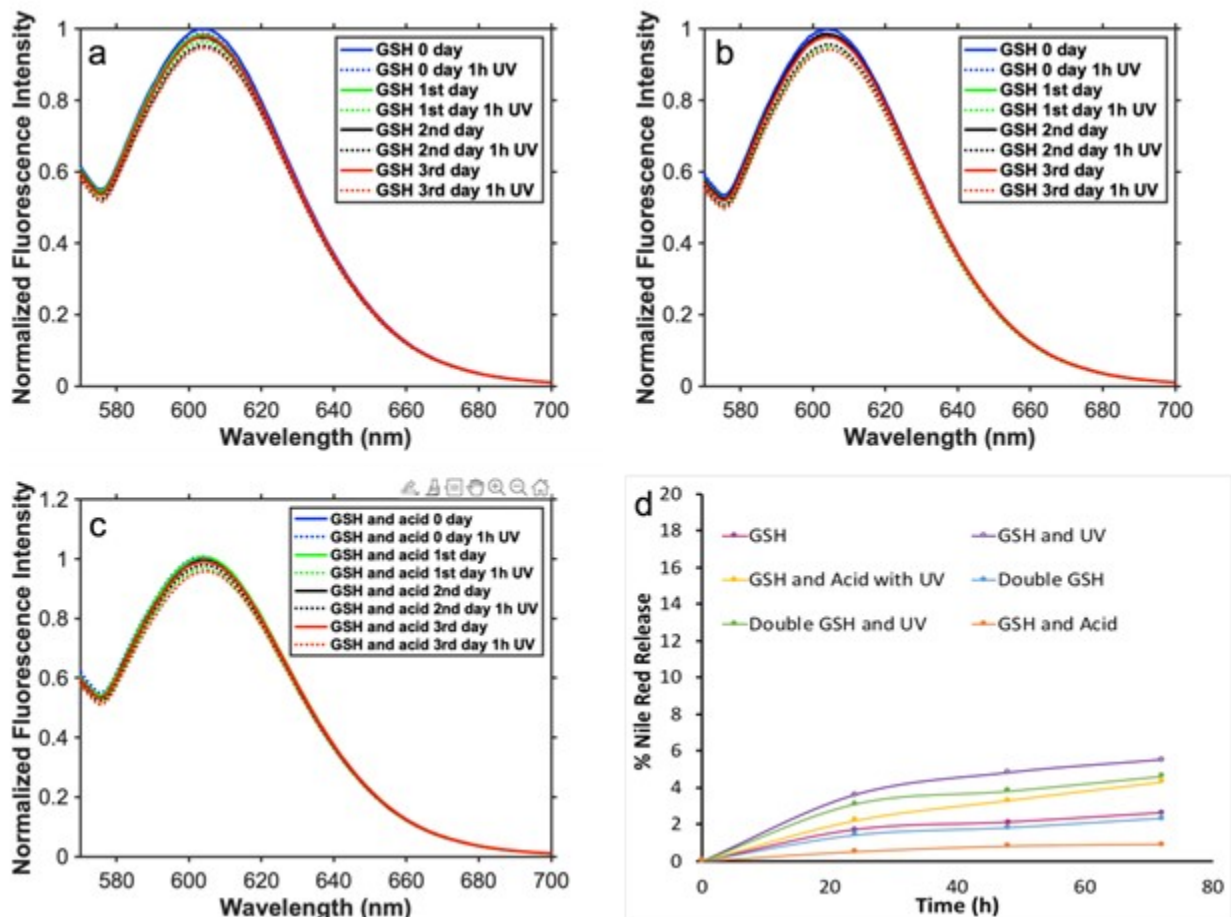


Figure S21. Fluorescence spectra of Nile Red loaded spherical TORC-NGs upon exposure to glutathione (GSH) at various concentrations. The molar ratios of GSH to CBMA are as follows: (a) GSH:CBMA = 64:1, (b) GSH:CBMA = 128:1. Additionally, the redox responsiveness was evaluated upon acidification to pH = 4 with HCl/H₂O at (c) GSH:CBMA = 64:1. The illustration (d) showcases the release pattern of spherical TORC-NGs in various environments in the presence of GSH.

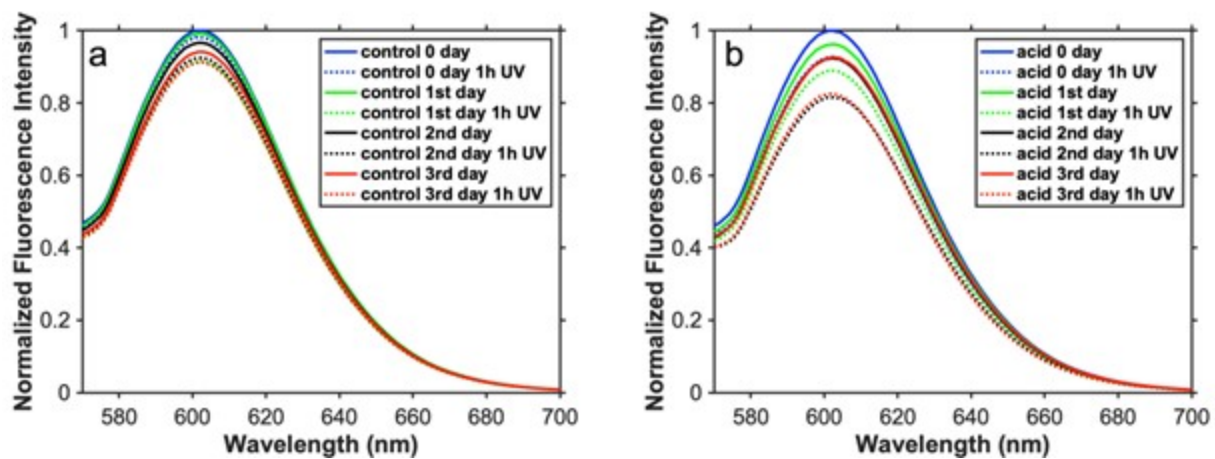


Figure S22. Fluorescence spectra of Nile Red loaded worm-like TORC-NG over the course of 3 days monitoring with (dotted lines) and without (solid lines) 254 nm UV irradiation at pH = 7 (a) and acidified to pH = 4 with HCl/H₂O.

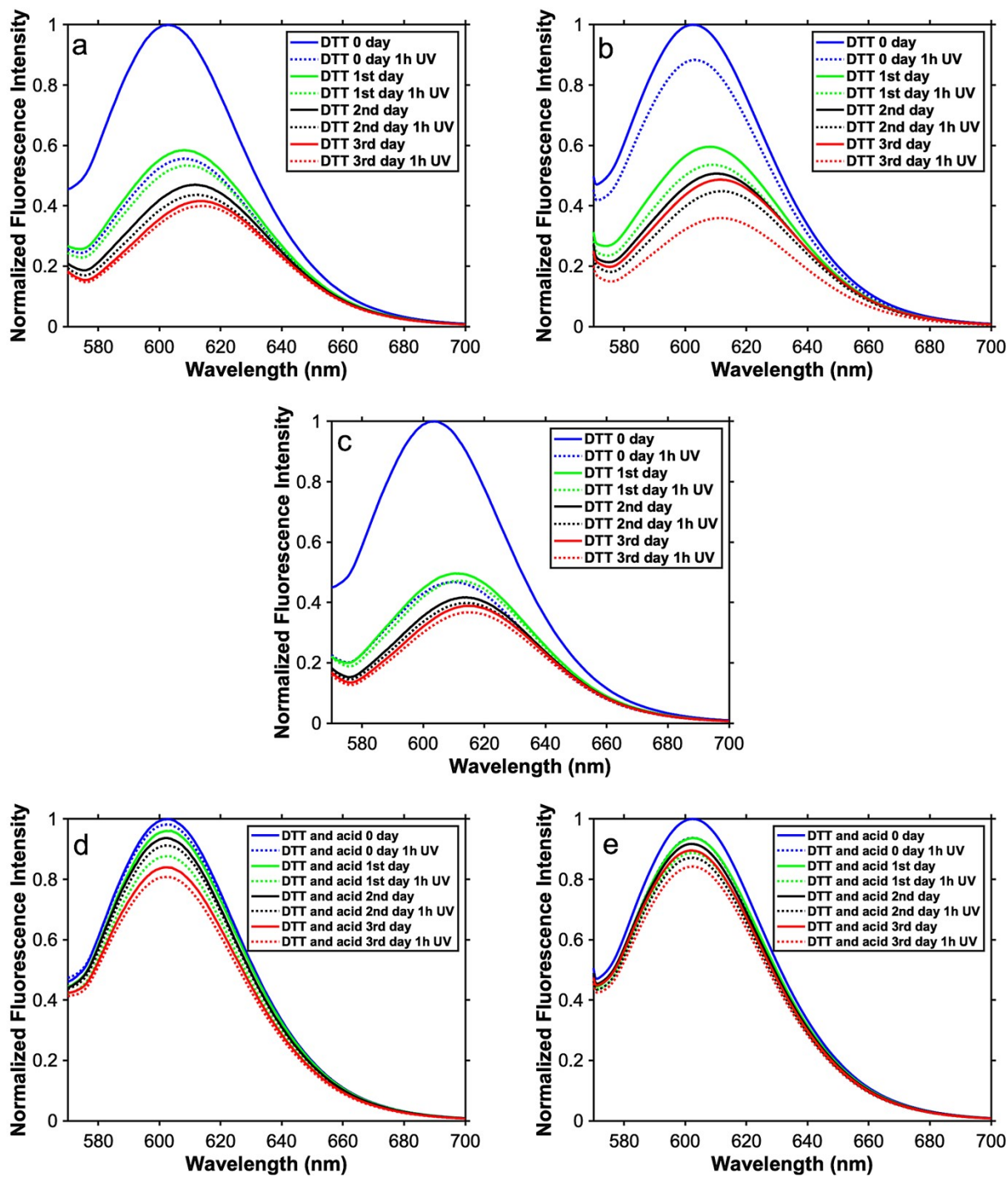


Figure S23. The fluorescence spectra of Nile Red loaded worm-like TORC-NGs upon exposure to dithiothreitol (DTT) at various concentrations. The molar ratios of DTT to CBMA are as follows: (a) DTT:CBMA = 64:1, (b) DTT:CBMA = 16:1, and (c) DTT:CBMA = 128:1. Additionally, the redox

responsiveness was evaluated upon acidification to pH = 4 with HCl/H₂O at two different DTT concentrations: (d) DTT:CBMA = 64:1 and (e) DTT:CBMA = 16:1.

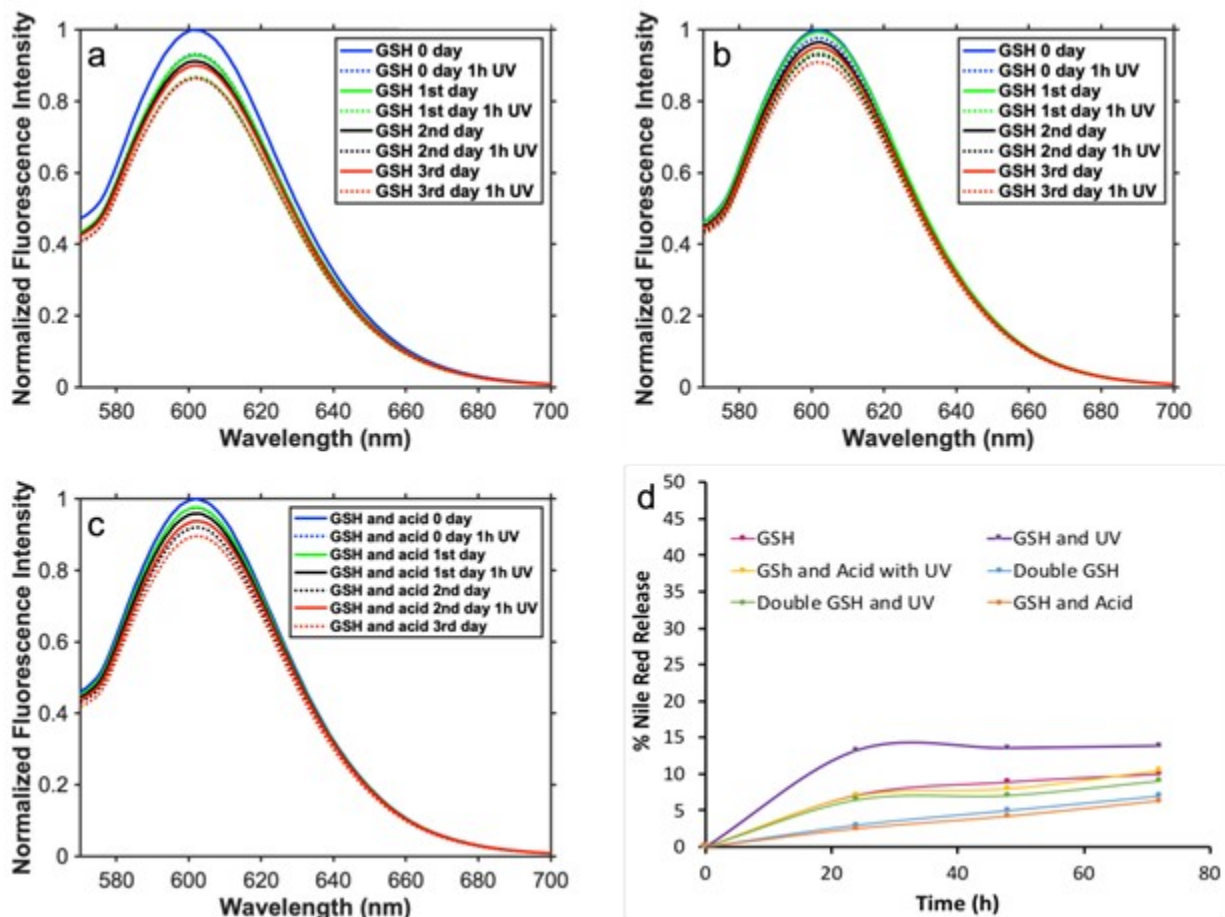


Figure S24. Fluorescence spectra of Nile Red loaded worm-like TORC-NGs upon exposure to glutathione (GSH) at various concentrations. The molar ratios of GSH to CBMA are as follows: (a) GSH:CBMA = 64:1, (b) GSH:CBMA = 128:1. Additionally, the redox responsiveness was evaluated upon acidification to pH = 4 with HCl/H₂O at (c) GSH:CBMA = 64:1. The illustration (d) showcases the release pattern of worm-like TORC-NGs in various environments in the presence of GSH.

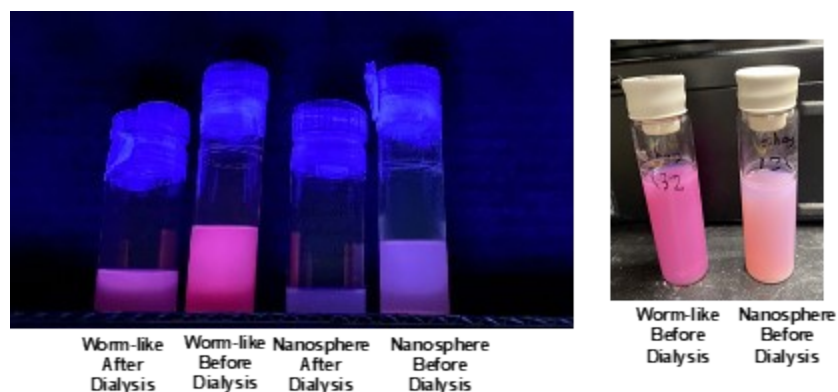


Figure S25. Photographs of Nile Red loaded TORC-NGs after polymerization before and after dialysis under UV light exposure in a black box (left) and under normal room light (right).

4.4. Cross-reactivity of PGMA Cores and DTT

The presence of reactive, nucleophilic thiol groups in DTT is hypothesized to potentially react with the reactive epoxide pendants leading to unwanted crosslinking reactions. To investigate this, an equivalent quantity of DTT was introduced to the non-CCL nanosphere control sample, and the epoxide chemical shifts and observed morphology changes were monitored using ^1H NMR and TEM analyses, respectively. ^1H NMR analysis revealed the disappearance of epoxide chemical shifts at (2.6 and 2.8 ppm (r), 3.6 and 4.25 ppm (d)) within 24h reacting and appearance of new peaks at 2.5 ppm, indicating the hypothesized ring-opening of epoxides using nucleophilic DTT thiols (**Figure S26**). Following these reactions, some gelation was observed which was analyzed using TEM showing agglomeration of nanomaterials as a result of the unwanted crosslinking of PGMA pendants (**Figure S27**).

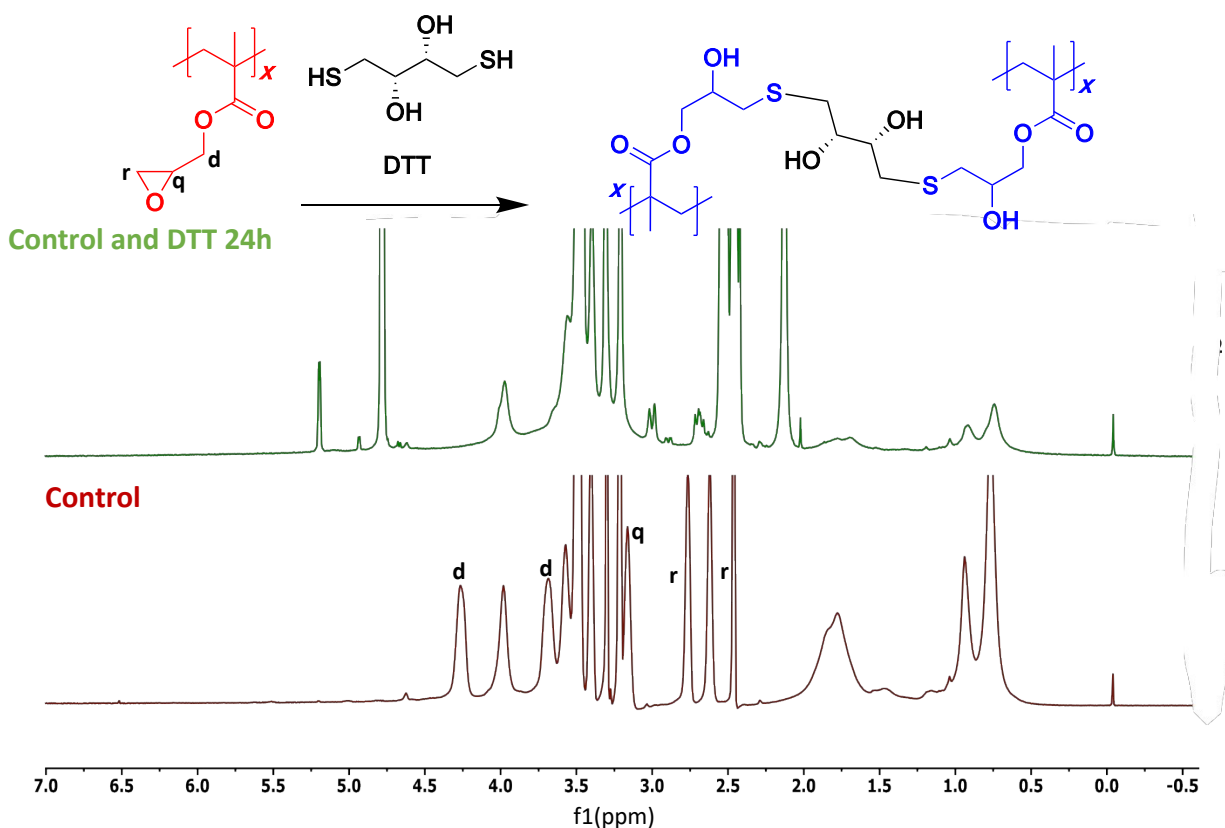


Figure S26. ^1H NMR spectra for non-CCL nanosphere controls demonstrating ring-opening $\text{S}_{\text{N}}2$ reactions with DTT which appear complete within 24h reaction.

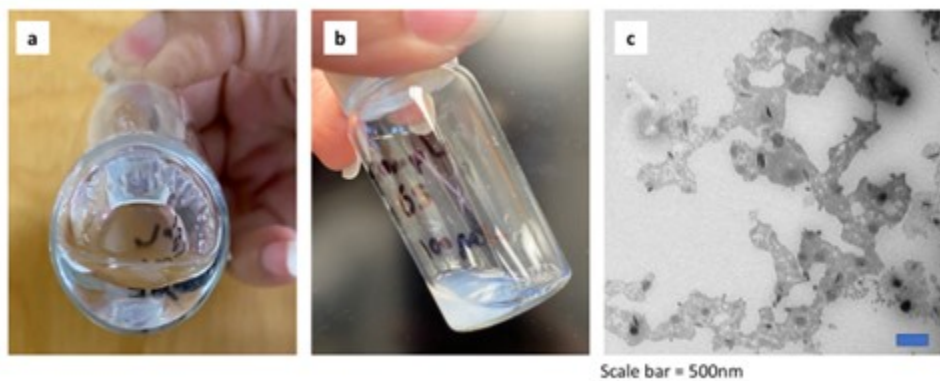


Figure S27. Photographs of reaction mixture and unwanted gel formation upon reaction between non-CCL nanospheres with DTT (a,b) and TEM image of aggregated morphologies within gel structure (c).

5. Sequential Application of Stimuli for AND-Gate release

In this section, fluorescence spectra associated with Nile Red release in the presence of different stimuli applied in various orders are displayed. Further, the effect of different pH (i.e., pH = 4, 7 and, 9) on release profile was investigated. The resulting, normalized fluorescence spectra are shown below along with plots for Nile Red release profiles.

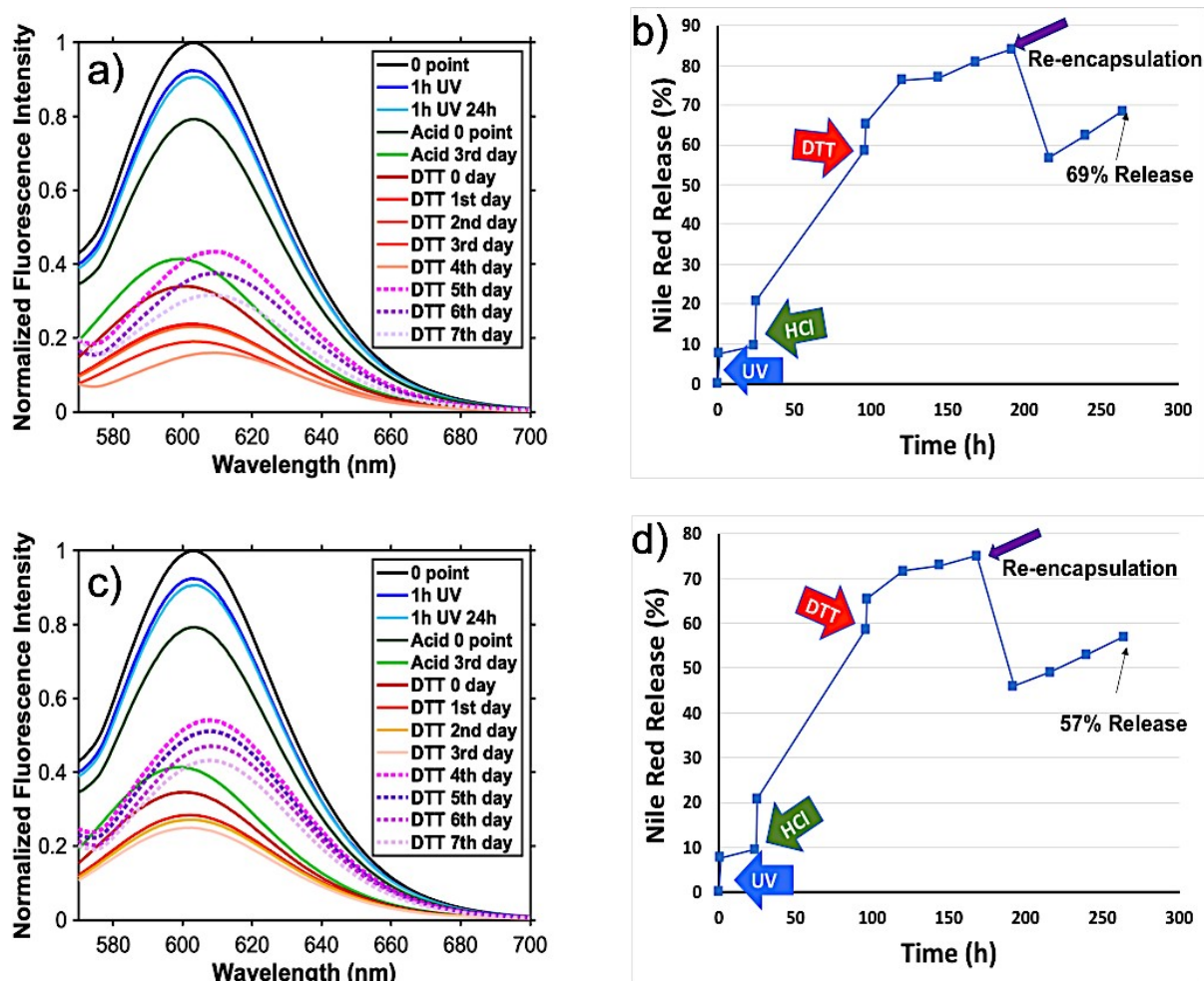


Figure S28. Fluorescence spectra and release profiles of Nile Red loaded worm-like TORC NGs after sequential application of UV, HCl and DTT stimuli over the course of 10 days. The stimuli were applied in the following order: 1) 1h 254 nm UV light irradiation, 2) acidification to pH = 4 with HCl/H₂O for 3 days, 3) DTT added at pH = 7 (a, b) or pH = 9 (c, d).

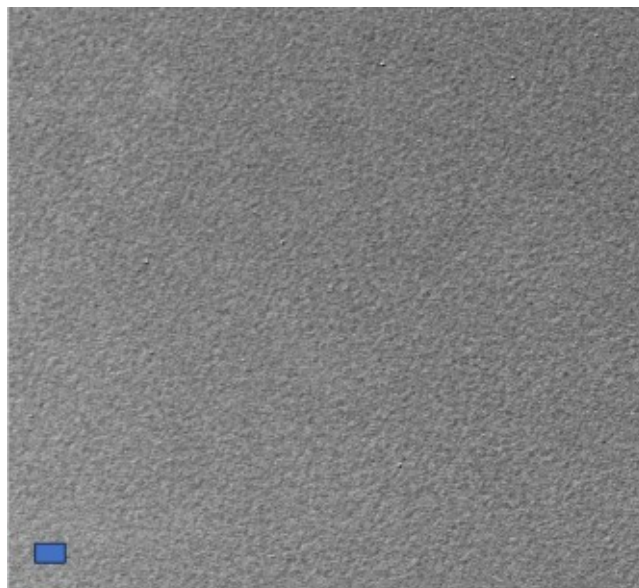


Figure S29. TEM image of disassembled nanosphereTORC NG after sequential addition of different stimuli at pH = 4 (scale bar = 500nm).

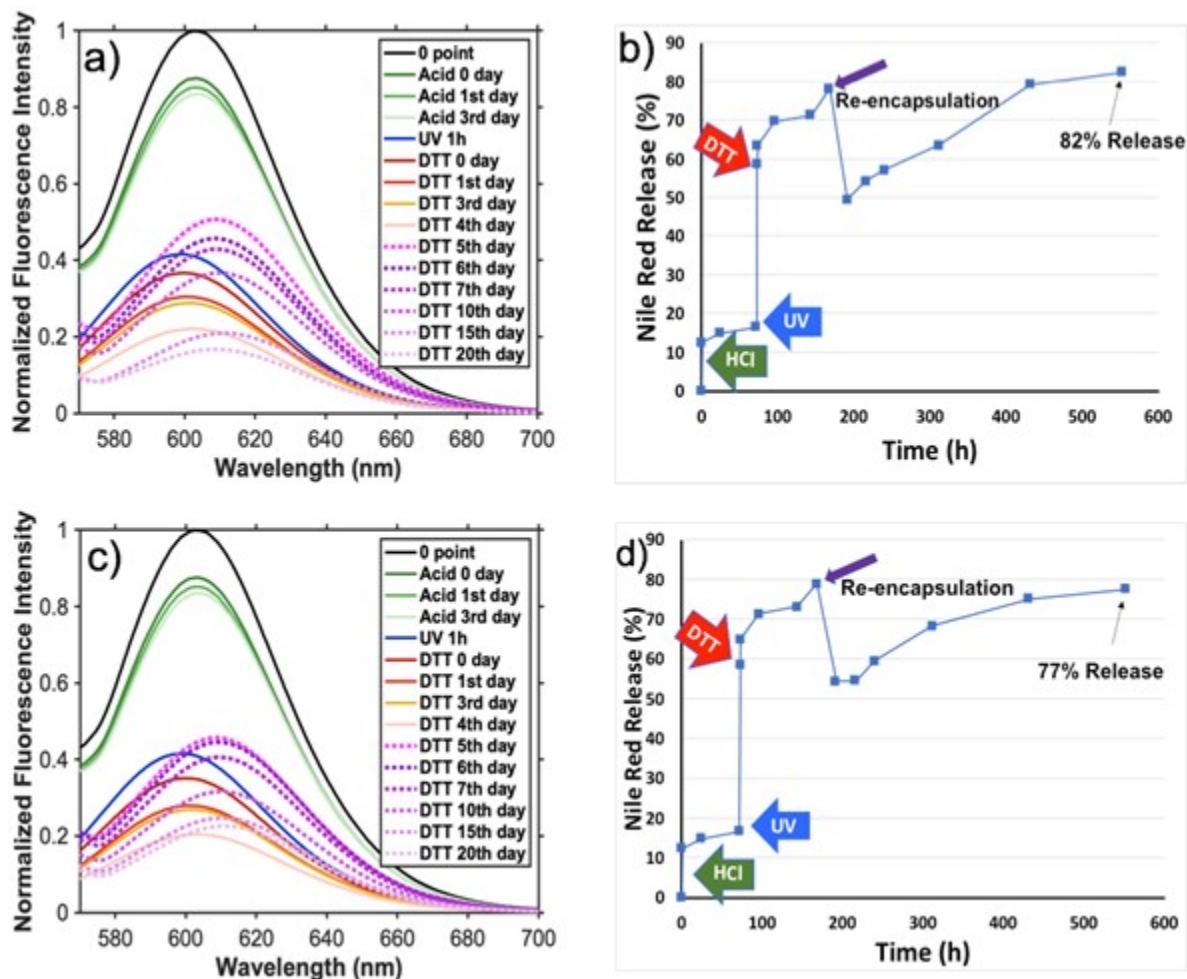


Figure S30. Fluorescence spectra and release profiles of Nile Red loaded worm-like TORC NGs after sequential application of UV, HCl and DTT stimuli over the course of 23 days. The stimuli were applied in the following order: 1) acidification to pH = 4 with HCl/H₂O for 3 days, 2) 1h 254 nm UV light irradiation, 3) DTT added at pH = 7 (a, b) or pH = 9 (c, d).

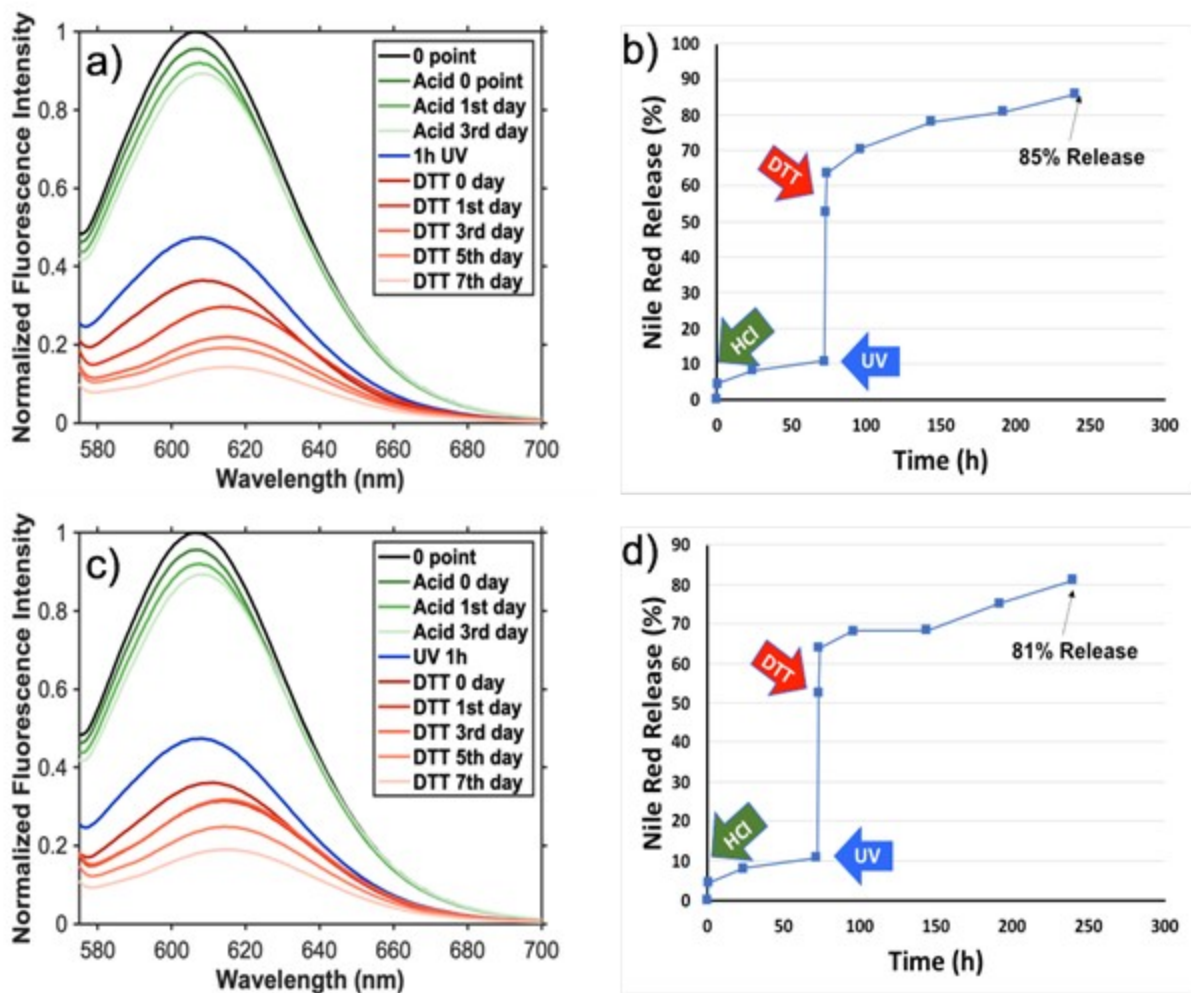
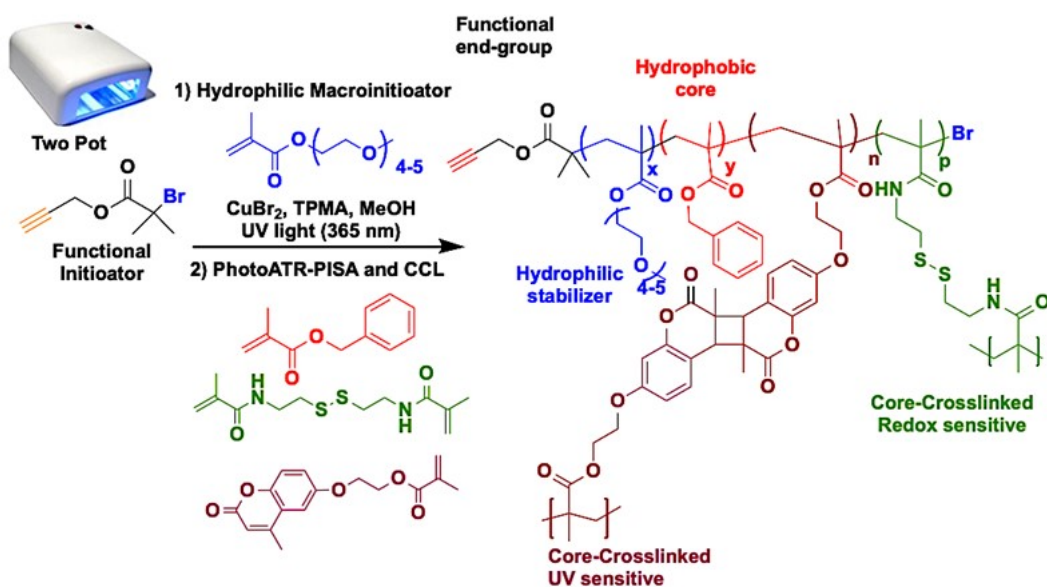


Figure S31. Fluorescence spectra and release profiles of Nile Red loaded spherical TORC NGs after sequential application of UV, HCl and DTT stimuli over the course of 10 days. The stimuli were applied in the following order: 1) acidification to pH = 4 with HCl/H₂O for 3 days, 2) 1h 254 nm UV light irradiation, 3) DTT added at pH = 7 (a, b) or pH = 9 (c, d).

6. Characterization and Nile Red Release for Tubesome TORC-NGs



Scheme S1. Synthesis of Nile Red encapsulated, tubesome TORC-NGs using poly(benzyl methacrylate) (PBMA) core-forming blocks.

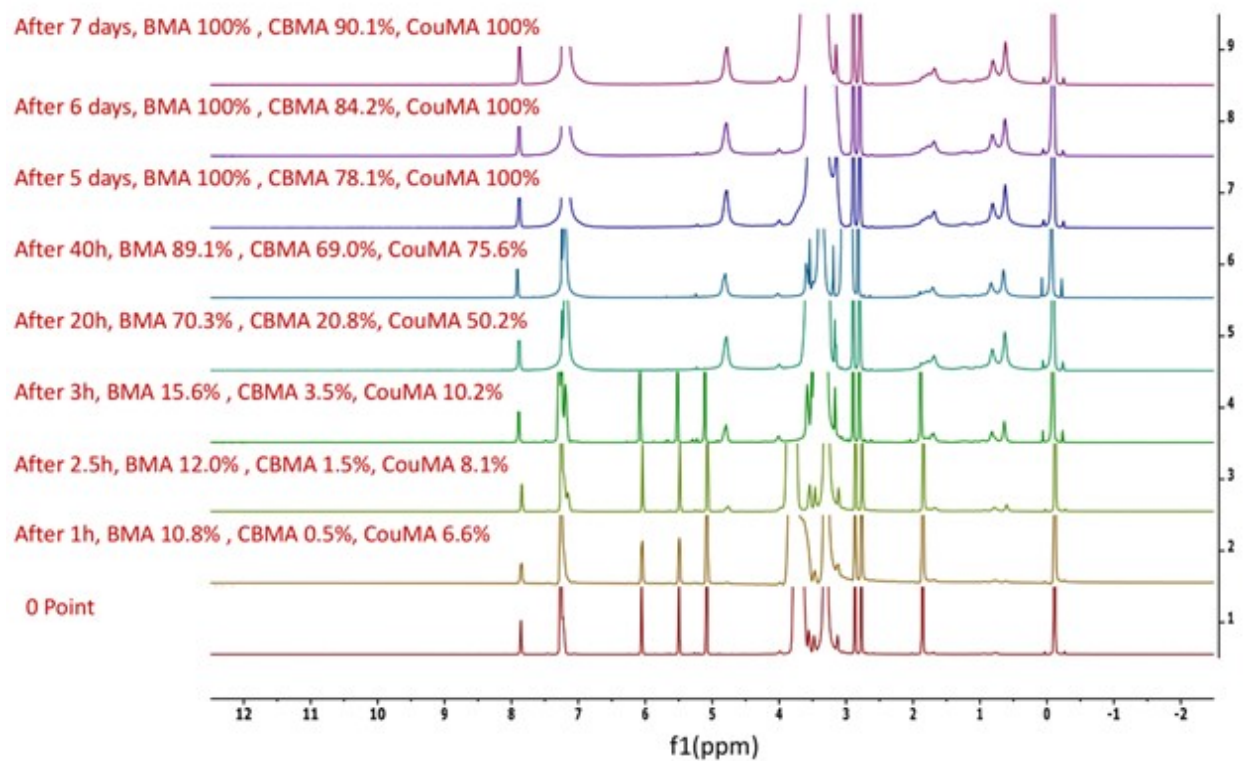


Figure S32. The progress of BMA and crosslinker conversion monitored using ^1H NMR spectroscopy over a period of 7 days. The obtained results indicated complete conversion for BMA, and conversions of 100% and 90% for CouMA and CBMA, respectively.

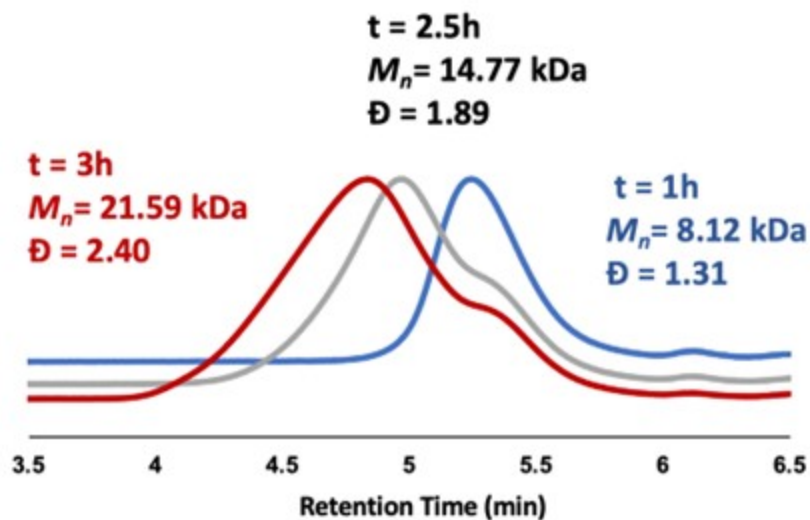


Figure S33. GPC chromatograms of block copolymerization of POEGMA-b-PBMA showing clear transitions to higher MW upon decreases in retention time.

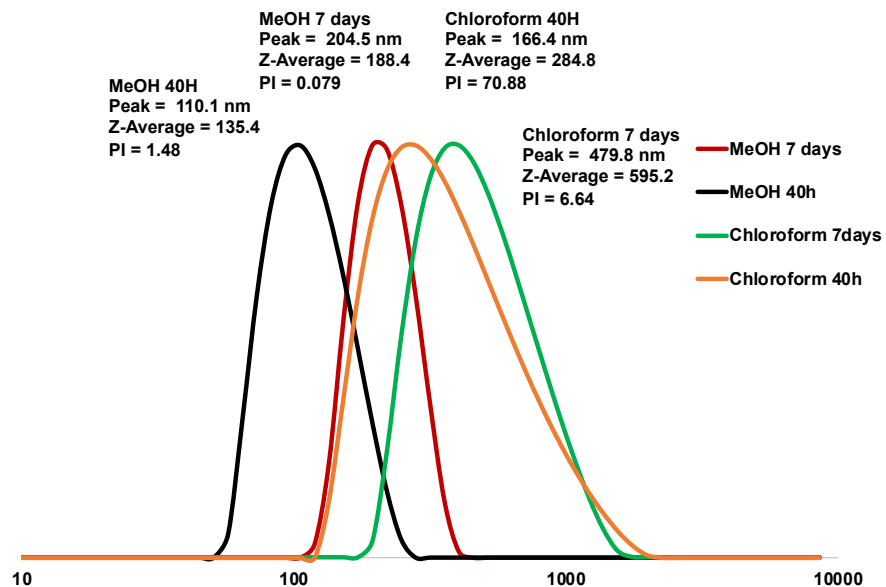


Figure S34. DLS of tubosome TORC-NGs after 40 h and 7 days reaction showing clear increases in hydrodynamic size and nanostructure stability upon solvent switches to CHCl_3 .

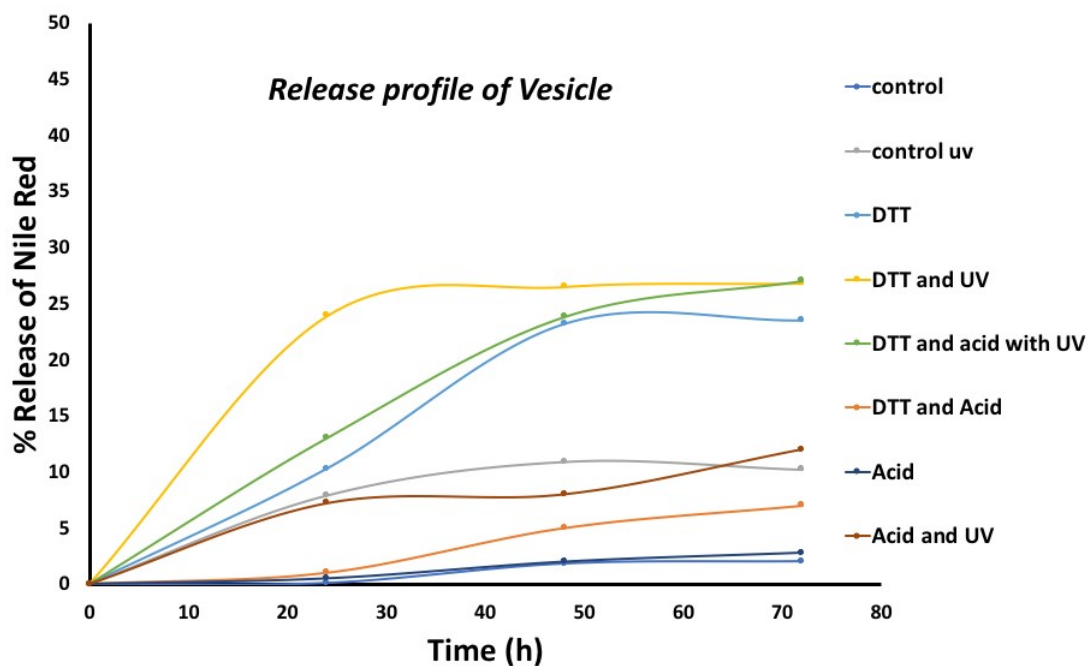


Figure S35. Release profile of Nile Red from tubosome TORC-NGs as calculated using fluorescence spectroscopy.

7. References

1. J. Dou, R. Yang, K. Du, L. Jiang, X. Huang and D. Chen, *Polymer Chemistry*, 2020, **11**, 3296-3304.
2. A. Shahrokhinia, R. A. Scanga, P. Biswas and J. F. Reuther, *Macromolecules*, 2021, **54**, 1441-1451.
3. A. Shahrokhinia, S. Rijal, B. Sonmez Baghirzade, R. A. Scanga, P. Biswas, S. Tafazoli, O. G. Apul and J. F. Reuther, *Macromolecules*, 2022, **55**, 3699-3710.